THE JOURNAL OF BIOLOGICAL CHEMISTRY
Vol. 275, No. 16, Issue of April 21, pp. 11771–11777, 2000

Printed in U.S.A.

Organization of Diphtheria Toxin in Membranes

A HYDROPHOBIC PHOTOLABELING STUDY*

(Received for publication, January 5, 2000, and in revised form, January 29, 2000)

Patrick R. D'Silva and Anil K. Lala‡

From the Biomembrane Laboratory, Department of Chemistry and Biotechnology Center, Indian Institute of Technology Bombay, Powai, Bombay 400 076, India

Diphtheria toxin (DT) is a disulfide linked AB-toxin consisting of a catalytic domain (C), a membrane-inserting domain (T), and a receptor-binding domain (R). It gains entry into cells by receptor-mediated endocytosis. The low pH (~5.5) inside the endosomes induces a conformational change in the toxin leading to insertion of the toxin in the membrane and subsequent translocation of the C domain into the cell, where it inactivates protein synthesis ultimately leading to cell death. We have used a highly reactive hydrophobic photoactivable reagent, DAF, to identify the segments of DT that interact with the membrane at pH 5.2. This reagent readily partitions into membranes and, on photolysis, indiscriminately inserts into lipids and membrane-inserted domains of proteins. Subsequent chemical and/or enzymatic fragmentation followed by peptide sequencing allows for identification of the modified residues. Using this approach it was observed that T domain helices, TH1, TH8, and TH9 insert into the membrane. Furthermore, the disulfide link was found on the *trans* side leaving part of the C domain on the *trans* side. This domain then comes out to the *cis* side via a highly hydrophobic patch corresponding to residues 134–141, originally corresponding to a β-strand in the solution structure of DT. It appears that the three helices of the T domain could participate in the formation of a channel from a DT-oligomer, thus providing the transport route to the C domain after the disulfide reductase separates the two chains.

There are several bacterial toxins that act by modification of intracellular substrates. Despite the fact that the structure of many of these toxins is now known, the mechanism of entry of these toxins into cells is far from clear (1–3). One of the major problems associated with getting an insight into the mechanism of entry is the very limited availability of information on the structure of membrane-bound toxins. Therefore, although diphtheria toxin (DT)[1] is an extensively studied protein toxin, a detailed mechanism of entry still eludes us. DT consists of two chains, A and B, that are joined by a disulfide link and is composed of three structural domains: the NH_2-terminal catalytic domain C (residues 1–193), transmembrane domain T (residues 205–378), and receptor-binding domain R (residues 386–535) (4, 5). DT enters cells by moving into the endosomal compartment using receptor-mediated endocytosis. The lowering of pH in the endosomes results in insertion of the toxin into the membrane and subsequent translocation of the A-chain into the cytosol, where it ADP-ribosylates the elongation factor-2, leading to inhibition of protein synthesis and eventual cell death (6–11). The T domain of DT is said to be primarily responsible for membrane insertion, though other domains, C and R, have also been shown to be associated with membranes (12–21). The T domain, comprised of three layers of helices with the innermost layer consisting of two hydrophobic helices TH8 and TH9, has been a subject of a number of studies involving interaction of this domain with single-bilayer vesicles at low pH (22–28). Although results obtained from these studies have been useful in pointing to pH-dependent insertion of TH8 and TH9 helices in membranes and location of the interhelical loop on the *trans* face of the membrane, many of these studies have been conducted with the T domain isolated (13, 29–32).

Hydrophobic photolabeling provides a promising approach to identification of membrane-associated segments of soluble proteins that enter membranes. This approach involves the use of a hydrophobic photoactivable reagent that partitions into membranes and on photolysis labels the membrane-spanning domains of transmembrane proteins. However, in the absence of any membrane, *i.e.* in solution, they can also be used to map hydrophobic surfaces in proteins. We report here our results on hydrophobic photolabeling of diphtheria toxin when it is bound to membranes with diazofluorene (DAF). This reagent readily partitions into membranes and on photolysis generates a highly reactive carbene, which labels the membrane-spanning domains of transmembrane proteins (33, 34). Analysis of photolabeled DT led to identification of membrane-associated segments of DT, thus permitting us to build a model of membrane-associated DT. Our results indicate that, besides the TH8 and TH9 helices, other parts of the T and C domains, namely, the TH1 helix of the T domain and the CB6 β-strand of the C domain, are associated with the membrane. Finally, the intrachain disulfide bond was observed to be on the *trans* side.

MATERIALS AND METHODS

Spectral grade water was obtained using Milli-Q Plus (Water Millipore, Bedford, MA). Tritiated fluorenone was obtained by catalytic

* This work was supported by a grant-in-aid from the Department of Science and Technology. The protein sequencing was carried out under a National facility for protein sequencing supported by Department of Science and Technology, and Department of Biotechnology. The costs of publication of this article were defrayed in part by the payment of page charges. This article must therefore be hereby marked "*advertisement*" in accordance with 18 U.S.C. Section 1734 solely to indicate this fact.

‡ To whom correspondence should be addressed. Biomembrane Laboratory, Department of Chemistry and Biotechnology Center, Indian Institute of Technology of Bombay, Powai, Bombay 400 076, India. Tel.: 91-22-5784383; Fax: 91-22-5767152; E-mail: anillala@chem.iitb.ernet.in.

[1] The abbreviations used are: DT, diphtheria toxin; DAF, [2-^{3}H]diazofluorene; PAGE, polyacrylamide gel electrophoresis; C domain, catalytic domain; T domain, transmembrane domain; R domain, receptor domain; DOPC, dioleoylphosphatidylcholine; DOPG, dioleoylphosphatidylglycerol; Tricine, *N*-[2-hydroxy-1,1-bis(hydroxymethyl)ethyl]glycine; CAPS, 3-(cyclohexylamino)propanesulfonic acid; PVDF, polyvinylidene difluoride; PTH, phenylthiohydantoin; RP-HPLC, reverse phase high performance liquid chromatography; DTT, dithiothreitol; SUV, single unilamellar vesicles.

tritium exchange of 2-iodofluoren-9-one, at BRIT (Bombay). [2-^{3}H]DAF (specific activity, 570 mCi/mmol) was prepared from [2-^{3}H]fluorenone according to the procedure reported earlier (35, 36). Mutated diphtheria toxin strain (pET.15bψ WTDT in BL-21) with a single E148S mutation was purified essentially according to a reported procedure (37). The concentration of DT was estimated according to the procedure of Lowry *et al.* (38). Dioleoylphosphatidylcholine (DOPC) and dioleoylphosphatidylglycerol (DOPG) was synthesized according to reported procedure (39, 40) and stored as chloroform solution at −20 °C. The phospholipid content was measured by phosphate assay (41). 20 mM Tris buffer (pH 7.4), containing 20 mM sodium acetate, or ammonium acetate buffer (pH 5.2), containing 150 mM NaCl, were used for all experiments unless specified otherwise. Automated Edman degradation of photolabeled peptides was carried out using a Shimadzu gas-phase protein sequencer (PPSQ10) connected to an on-line phenylthiohydantoin analyzer. The samples were loaded either as electroblots on a polyvinylidene difluoride (PVDF) membrane or on glass fiber disks. High performance liquid chromatography (HPLC) analysis was carried out on a Shimadzu LC-10A system. Sonicated SUVs (single unilamellar vesicles) were used in all experiments. To prepare sonicated SUVs, appropriate concentrations of stock solution of 30% DOPG and 70% DOPC in $CHCl_3$ were added to a glass tube, dried under argon or nitrogen gas, and then further dried under high vacuum for 8 h. The dried film was hydrated in 1 mL of degassed buffer with vortexing. The suspension was sonicated on ice using a sonifier (Branson Model B-30) until nearly optically clear. The resulting clear solution was spun at 15,850 × *g* to remove any titanium particles shed from the microtip during sonication. The SUVs were freshly prepared for all experiments.

CNBr Fragmentation of Membrane-bound Photolabeled DT and Analysis of Fragments—5 nmol of membrane-bound photolabeled-DT was subjected to CNBr fragmentation in 70% formic acid. The CNBr digest of photolabeled DT was run on a 16.5% Tris-Tricine gel system (42) and immediately electroblotted onto a PVDF membrane using 10 mM CAPS containing 30% methanol in transfer buffer (43). The PVDF membrane was stained for 1 min in 0.1% Coomassie Blue and destained in 50% methanol/water. Five bands corresponding to the molecular masses of the fragments CN-2, CN-3, CN-5, CN-8, and CN-9 were clearly visible on the PVDF membrane. The radioactive bands were excised and analyzed by sequencing in an automated gas-phase protein sequencer. Similarly 60 μg (1 nmol) of photolabeled vesicle-bound DT was analyzed on 12% SDS-polyacrylamide gel electrophoresis (PAGE) to separate A and B chains followed by electroblotting as described above. The B-chain was subjected to Edman degradation.

Isolation of the CN-7 Fragment (315–339) by Reverse Phase-HPLC—The CNBr digest of membrane-bound photolabeled DT (120 μg, 2 nmol) was dissolved in 20% formic acid and separated by reversed phase (RP)-HPLC on a Vydac C_4 column (4.6 × 150 mm). A gradient of acetonitrile containing 0.1% (v/v) trifluoroacetic acid from 0 to 15% in 5 min, 15 min (15–30%), 45 min (30–60%), 55 min (60–80%), and finally 80% acetonitrile for 10 min, was used. The flow rate was kept at 0.8 mL/min, the eluate was monitored at 216 nm, and fractions were at 1-min interval were collected. The fractions eluting between 19 and 21 min were pooled and concentrated. This fraction, which was identified as the CN-7 fragment by sequencing in an independent experiment, was dot-blotted on a methanol-treated PVDF membrane (washed with methanol for 5 s and then washed with water for 1 min) and dried completely for 4 min at 50 °C. The dot blot was thoroughly washed with water to remove acetic acid and subjected to sequencing in an automated gas-phase protein sequencer.

Endoproteinase Glu-C Digestion—180 μg (3 nmol) of membrane-bound photolabeled DT, isolated by gel-permeation column chromatography as described in the legend to Fig. 1, was subjected to endoproteinase Glu-C digestion. The proteolysis was performed in 20 mM ammonium acetate buffer, containing 150 mM NaCl, pH 5.2. Freshly prepared endoproteinase Glu-C (25% w/w) was added, and the whole preparation was incubated at 37 °C for 6 h. After 6-h digestion, additional protease (25% w/w) was added and incubated for the next 20 h. The released peptides and vesicle-bound residual toxin were separated by passing once again over a gel-permeation HPLC column. The void volume fraction corresponding to vesicle-bound proteolyzed toxin was concentrated and subjected to delipidation followed by trichloroacetic acid precipitation as mentioned in the legend to Fig. 1. The membrane-bound fragments so isolated were then analyzed on 16.5% Tris-Tricine gel and electroblotted on a PVDF membrane. There were large numbers of membrane-bound fragments that could be visualized on staining with Coomassie Blue and, based on their molecular masses, were found to be similar to that reported earlier (44). Many of these bands, which were blotted onto the PVDF membrane, were identified by peptide sequencing. The band corresponding to approximately 14 kDa was subjected to the Edman degradation. A single peptide beginning with Leu^{263} (LKTVT . . .) was detected. Sequencing could be carried out for 26 cycles, and the radioactivity release was monitored for each cycle.

Isolation of A-chain from Membrane-bound Photolabeled DT and Cleavage by o-Iodosobenzoic Acid—480 μg (8 nmol) of photolabeled membrane-bound DT was separated on preparative 12% SDS-PAGE Laemmli gels. The band corresponding to A- and B-chains was sliced from the gel and subjected to elution using a sonication extraction procedure (45). The bands were washed five times (10 min) with 5 mL of 250 mM Tris buffer containing 250 mM EDTA, pH 7.4, in Falcon tubes. The gel pieces were then washed five times with 5 mL of water. Finally, the gel pieces were crushed with a glass rod. The gel homogenate was resuspended in 2 mL of 20 mM Tris buffer, pH 7.4, containing 0.1% SDS. The samples were sonicated for 3 min, in an ice bath with a Branson B-30 probe sonicator. Samples were centrifuged in a microcentrifuge, and the supernatant was passed over 2 mL of Sephadex G-25 equilibrated with 20 mM Tris buffer, pH 7.4. The eluate was lyophilized, and protein recovery was found to be 80% as estimated by Lowry assay.

125 μg of A-chain was dissolved in 100 μL of 12 mM phosphate buffer, pH 6.5, containing 4 M guanidine-HCl. This solution was then treated with a 2.5 M excess of *o*-iodosobenzoic for 30 min and followed by lyophilization. The lyophilized sample was dissolved in 200 μL of 80% acetic acid containing 4 M guanidine-HCl and incubated for 20 h at 25 °C in the dark. This sample was then desalted on a PD-10 column and lyophilized. The digest (80 μg) was analyzed on the 16.5% Tris-Tricine gel system (42) and immediately electroblotted onto a PVDF membrane using 10 mM CAPS buffer containing 35% methanol in transfer buffer (43). Four bands of 15-, 11-, 7-, and 4.5-kDa molecular mass were clearly visible on Coomassie Blue staining. The 11- and 4.5-kDa bands were subjected to Edman degradation. Similarly, 25 μg of the digest of A-chain was analyzed on the same gel, and radioactivity associated with different bands was estimated by slicing the gel, solubilizing, and counting.

RESULTS

In order to get structural information on membrane-associated DT, we partitioned DAF into DOPC-DOPG vesicles prepared at pH 5.2 and incubated with DT at a protein-to-lipid ratio of 1:250, leading to insertion of the latter in vesicles as confirmed by independent experiments. The whole preparation was then photolyzed and subjected to gel-permeation chromatography, and free DT was separated from the DT-bound vesicles. Under the experimental condition used, more than 80% of DT was bound to vesicles (Fig. 1). Furthermore, the DT-bound vesicles were found to be stable at pH 5.2 for several hours and showed no signs of DT leaching from vesicles. Radioactive analysis of the eluant resulting from gel-permeation chromatography indicated that the bulk of the radioactivity was associated with vesicle-bound DT and not free DT (data not shown). However, because DAF is known to extensively label lipids also (34–36), vesicle-bound DT fractions were delipidated and subjected to SDS-PAGE analysis along with free DT fractions. Although both samples showed bands corresponding to A- and B-chains on staining with Coomassie Blue, radioactivity was found to be associated only with A- and B-chains of vesicle-bound DT (Fig. 1, *A* and *B*). These results clearly indicate that, owing to the high partition coefficient of DAF in favor of the membrane hydrophobic core (34–36), once DAF is partitioned into membranes it exclusively labels proteins associated with membrane and not soluble proteins that it would otherwise label in the absence of membranes. Further labeling of both A- and B-chain indicated that both chains insert into the membrane. This result is in agreement with previous studies (17, 18, 46).

CNBr Fragmentation of DT and Identification of Different Fragments—DT has 8 well-spread methionine residues (14, 115, 178, 182, 230, 314, 339, 459), which provide useful fragments for identification of DAF-modified sites by sequence analysis. These fragments could be separated by SDS-PAGE on Tris-Tricine gels, followed by electroblotting onto a PVDF membrane and Edman degradation. The molecular mass and

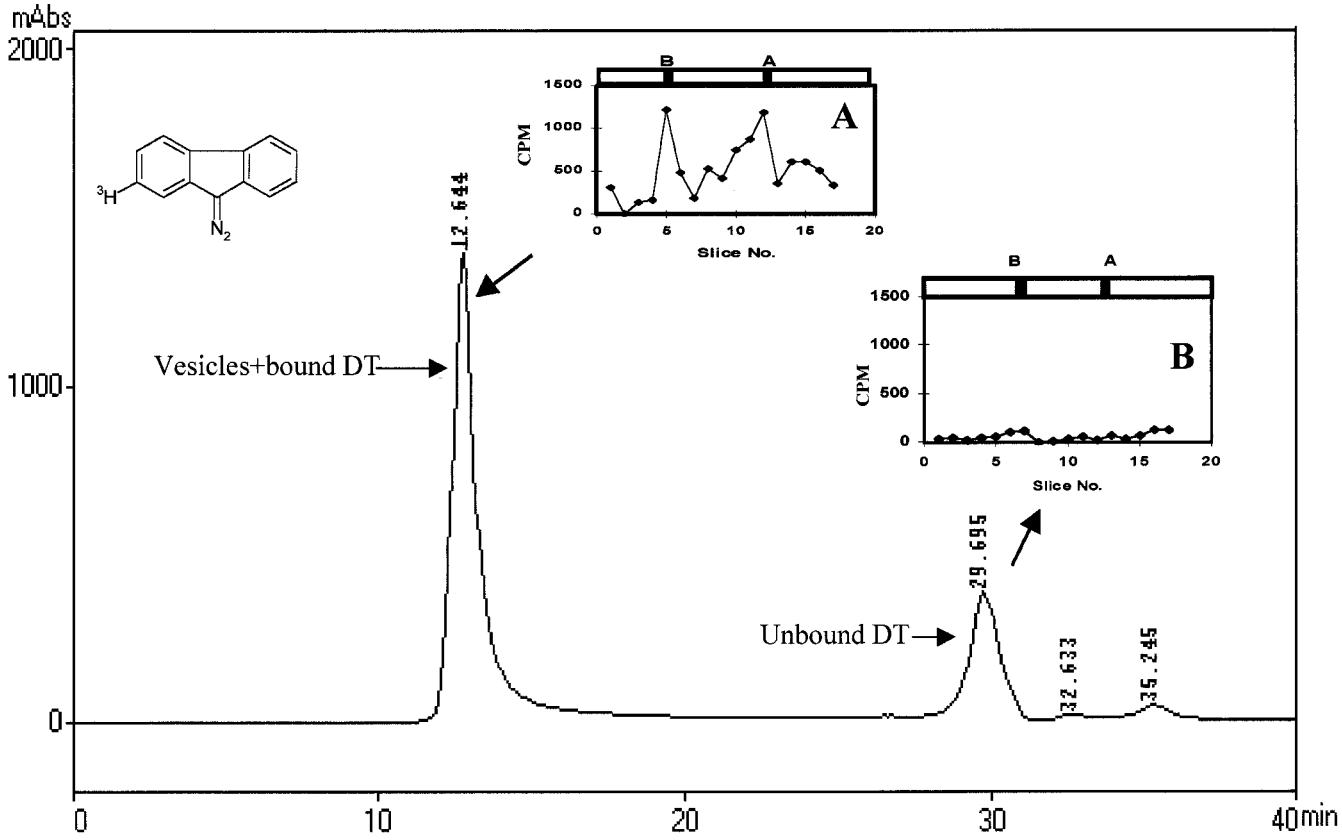

FIG. 1. **Isolation of membrane-bound DT by gel-permeation HPLC and SDS-PAGE analysis.** An ethanolic solution of [^{3}H]DAF (*inset*, *top left*) (2 μCi, 2.5 nmol) was added to DOPC/DOPG (70:30, v/v) vesicles (1.25 mM final lipid concentration) prepared by sonication in 20 mM sodium acetate buffer containing 150 mM NaCl, pH 5.2, and incubated for 30 min in the dark. The total alcohol concentration was always below 2% (v/v). The final concentration of [^{3}H]DAF was 25 μM. DT (300 μg/mL) was then added and incubated for 60 min. At the end of 1 h, the tubes were photolyzed for 2 min using a Rayonet Minireactor with four 3000-Å lamps at a distance of 6 cm from the sample tube. In a control experiment, the sample was not photolyzed. Unreacted [^{3}H]DAF, if any, was destroyed by the addition of glacial acetic acid to a final concentration of 0.3 M. The photolyzed sample was passed over a gel-permeation HPLC column TSK G-3000 SW (7.5 × 600 mm), equilibrated with the 20 mM sodium acetate buffer containing 150 mM NaCl, pH 5.2, and eluted at a flow rate of 0.8 mL/min. The elution was monitored at 220 nm. The positions of DT and free vesicles were first typed under same conditions. The peak area of unbound DT was used to quantify unbound DT using a standard curve. The DT-bound vesicles (R_t 12.6 min) and free DT (R_t 29.7 min) were then collected, concentrated to dryness, suspended in samples in 100 μL of water, and subjected to delipidation using chloroform:methanol (1:1). The aqueous layer was subjected to precipitation with trichloroacetic acid. After addition of trichloroacetic acid (10% final concentration), the suspension was cooled for 30 min over ice. The pellet was then washed three times with cold acetone, dissolved in SDS sample buffer and analyzed on a 12% SDS-PAGE according to the procedure of Laemmli (58). The gel was stained in 0.1% Coomassie Blue and destained. The gel was then sliced into 2-mm pieces and digested into 250 μL of 30% H_2O_2 at 60 °C for 8–10 h. The digested samples were counted in a toluene-based scintillation mixture. The *inset* (*A*, *B*) shows SDS-PAGE analysis of vesicle-bound and unbound DT. The *schematic* at the top of the gel gives the Coomassie Blue staining pattern and the positions of A- and B-chains.

NH_2-terminal sequence analysis permitted identification of CN-2 (15–115, ENFSSYHG . . .), CN-3 (116–178, EQVGTEEF . . .), CN-5 (NH_2 terminus of B-chain, 194–230, SVGGSSLS . . .), CN-8 (340–459, VAQAIPLV . . .), and CN-9 (460–535, RCRAIGD . . .).

CNBr Fragmentation of Membrane-bound DT Labeled by DAF and Sequencing—Because DAF photolabels only the membrane-embedded domains of transmembrane proteins (34, 35), DAF-labeled DT was subjected to CNBr fragmentation in an effort to get information on membrane-inserted domains of DT. The CNBr digest of DAF-labeled DT isolated from the vesicle fraction mentioned above was subjected to SDS-PAGE analysis (Fig. 2*A*), which indicated that the different fragments were labeled. The NH_2-terminal region of the CN-8 fragment corresponds to part of the two putative membrane-inserting hydrophobic helices TH8 (326–347) and TH9 (358–376) and the interlinking loop TL5 (348–357). Sequencing of this region indicated that, although 4 major residues belonging to TH9 (Ala^{356}, Phe^{360}, Leu^{367}, and Val^{371}) were labeled, no residue in the interlinking loop TL5 was labeled (Fig. 2*D*). This is consistent with the hypothesis that the TL5 loop is present on the *trans* side in the membrane-inserted state of DT (9, 24, 32). In order to obtain insertion site information on the other helix, TH8, CN-7 (315–339) was obtained by RP-HPLC analysis of the CNBr fragments on a C4 column. Sequencing of CN-7 indicated extensive labeling of Ala^{320}, Ile^{328}, Val^{329}, Ile^{333}, Gln^{342}, Ala^{343}, Ile^{344}, and Pro^{345} (Fig. 2*C*). A helical wheel representation of labeled residues in TH8 and TH9 indicated that primarily one side of the helices was labeled (Fig. 2*B*). This result, combined with the absence of labeling in the interlinking TL5 loop, suggest that these two buried hydrophobic helices found in the T domain of the solution structure of DT, insert into the membrane and maintain their helical motif. The sidedness of labeling seen in the helical wheel representation further suggests that the labeled sites correspond to the lipid-facing face of these helices in the membrane-associated state (Fig. 2*B*). However, the labeling of Ala^{320} suggests that regions beyond these helices also interact with the membrane.

The reduction of inter-chain disulfide link during sample preparation and CNBr fragmentation leads to a truncated CN-5 fragment (193–230) corresponding to the NH_2 terminus of the B-chain, which incorporates the TH1 (206–222) and TH2 (224–232) helices. The entire fragment was sequenced until 37 cycles. The major labeled residues correspond to Trp^{206}, Val^{208},

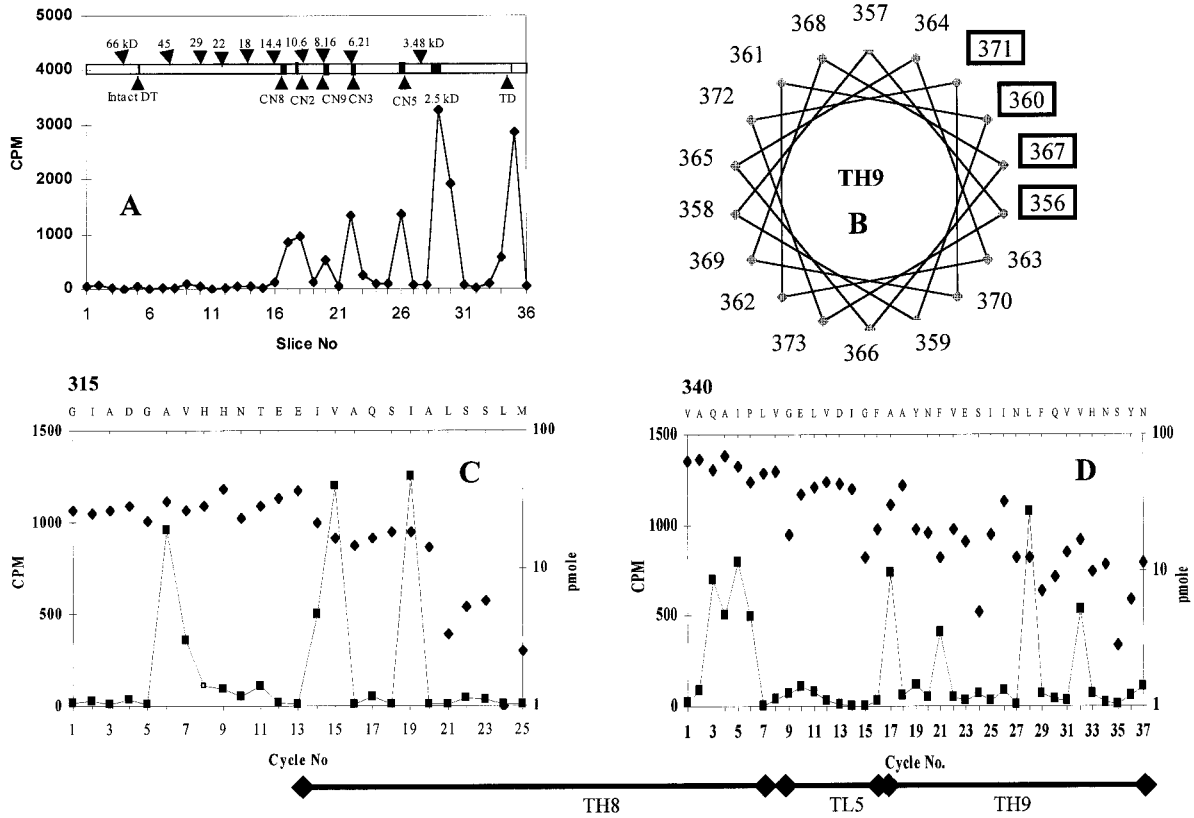

FIG. 2. *A*, Tris-Tricine gel for CNBr digest of membrane-bound DT. 30 μg of CNBr digest of photolabeled DT was separated on 16.5% Tris-Tricine gel, and radioactive analysis of the CNBr fragments was carried out by gel staining and solubilization, as described under "Materials and Methods." The *schematic* at the top gives the Coomassie Blue staining pattern, and the *arrowheads* indicate the positions of standard molecular mass markers and the CNBr fragments of DT. *B*, helical wheel representation of the TH9 helix (356–376). Only the first 18 residues are represented in the wheel. The residues labeled by DAF are enclosed in *boxes*. *C*, radioactivity and mass release on Edman degradation of CNBr fragment CN7 (315–339) of DAF-labeled DT. The CN7 fragment was isolated by RP-HPLC using a Vydac C4 column described under "Materials and Methods," dot blotted on a PVDF membrane, and subjected to Edman degradation. In each degradation cycle 60% of the sample was analyzed by direct injection using an on-line PTH analyzer for PTH-derivative release (picomoles, ♦). The remaining 40% of the sample was directed to a fraction collector and subsequently counted (cpm, ■). A single peptide beginning with glycine-315 was detected. The sequence assignments could be made up to 25 cycles and are given on the top. The position of part of the TH8 helix is indicated by the *arrowhead*. *D*, radioactivity and mass release on Edman degradation of the CNBr fragment CN-8 (340–459) of DAF-labeled DT. The band corresponding to the CN-8 fragment was subjected to Edman degradation. A single peptide beginning with valine-340 was detected. The sequence assignments could be made for up to 37 cycles and are given at the top. PTH-derivative release (picomoles, ♦) and radioactivity released in the sequencing cycle (cpm, ■) given at the top. The positions of part of the TH8 helix, the TL5 loop, and the TH9 helix are indicated by the *arrowhead* at the bottom.

Ile^{209}, Thr^{213}, Ile^{217}, and Leu^{220}. No residue was labeled in the sequence before or after the TH1 helix (Fig. 3*A*). These data suggest that only the TH1 helix interacts with the membrane. TH1 is an amphiphilic helix; it is interesting to see that only the residues on the lipid facing the hydrophobic side of the helix are labeled (Fig. 3*B*). The interaction of the TH1 helix with the membrane has been suggested earlier, although it has not been clear whether the helix lies on the membrane-water interface or transverses the membrane. Data in favor of the latter hypothesis have been growing recently (7, 9, 24, 44, 47). In such a membrane-transversing state TH1 could participate in a pore formation with the hydrophilic side forming the lumen of the pore. However, the inter-chain disulfide link has to be on the *trans* side in this topography. Our photolabeling data cannot discriminate between the two possible orientations of TH1. To get suitable answers to this important question, we subjected the vesicle-bound DT to reduction by dithiothreitol (DTT) at pH 7.4 and isolated it by gel-permeation chromatography. The sample was then delipidated and analyzed by SDS-PAGE under nonreducing conditions. The vesicle-bound DT was observed as a single band at 59 kDa corresponding to intact unreduced DT. In a control experiment where free DT was used, two bands corresponding to the A- and B-chains were observed (Fig. 3*C*). These experiments clearly indicated that the A- and B-chain inter-chain disulfide bridge is located on the *trans* side of the membrane and the TH1 helix transverses the membrane. Similar conclusions have been made earlier in planar lipid bilayer studies (48). Furthermore, the TH2 helix must be positioned on the extracellular side. Based on the *trans* localization of the inter-chain disulfide bridge, it can be argued that the A-chain must lie either fully inside the intracellular space or it must cross the membrane at least once to be present on the extracellular side. The sequencing of the CN-2 fragment could be carried out for 35 cycles, and it was observed that practically no residue became labeled (Fig. 3*E*). The sequencing of the CN-3 fragment could also be carried out for up to 35 cycles (Glu^{116}-Asn^{151}). However, in this part of DT, the region corresponding to Val^{134}-Ala^{141} was extensively labeled, with the rest of the region being unlabeled (Fig. 3*E*). An important and unique feature of this labeled region is that it corresponds to the β-sheet region (CB6) in the solution structure, and, if it were to transverse the membrane with the parent structural motif retained in the membrane-bound state, it would require about 10 residues as in the case of other β-strands. This is about the length of the labeled region, which is hydrophobic and is flanked on one side by Arg^{133} and Glu^{142} on the other side. Another noticeable feature of this region is that all labeled residues are contiguous and no periodicity of labeling is ob-

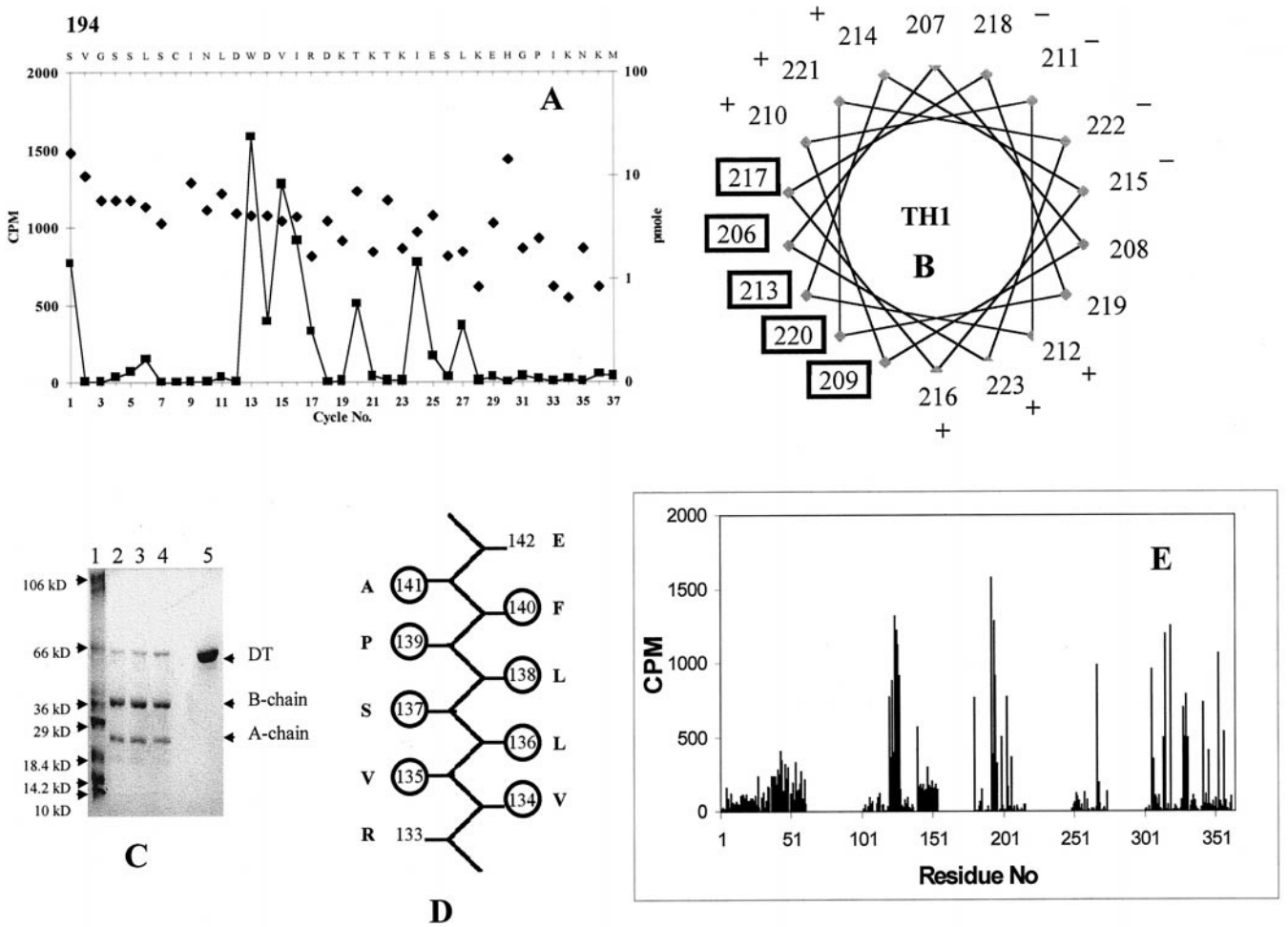

FIG. 3. *A*, radioactivity and mass release on Edman degradation of the NH_2 terminus of the B-chain of DAF-labeled DT. 60 μg of photolabeled DT was loaded onto 12% SDS-PAGE to separate the A- and B-chains followed by electroblotting as described under "Materials and Methods." The B-chain was subjected to Edman degradation. The sequence assignments could be made for up to 37 cycles and are given at the top. PTH-derivative release (picomoles, ♦) and the remaining 40% of the sample was directed to a fraction collector and subsequently counted (cpm, ■). Sequencing of the CN-5 fragment also gave similar results. *B*, helical wheel representation for TH1 (206–221). The residues labeled by DAF are enclosed in *boxes*. The + and − symbols refer to the charges on residues. *C*, SDS-PAGE of vesicle-bound DT and free DT in non-reducing sample buffer. 60 μg of DT incubated with DOPC/DOPG (1.25 mM final lipid concentration) in sodium acetate buffer, pH 5.2, and separated on a gel permeation column (legend to Fig. 1) was equilibrated with 20 mM Tris-buffer, pH 7.4, containing 0.15M NaCl. The void volume and elution volume were collected and incubated in the presence of an excess (200 M) of DTT in the same buffer used above at 23 °C for 3 h. The control experiment was carried out in the absence of vesicles. The excess DTT was removed by gel-filtration on a PD-10 column. The void volume was then subjected to delipidation followed by trichloroacetic acid precipitation as described in legend to Fig. 1. The sample was analyzed on 12% SDS-PAGE. All samples were analyzed under non-reducing conditions. *Lane 1*, standard molecular mass markers; *lane 2*, control (DT alone); *lane 3*, unbound DT; *lane 4*, membrane-bound DT. *D*, β-strand (133–142) of the CN-3 fragment. The residues labeled by DAF are enclosed in *circles*. The strand begins with Arg (133) and ends with Glu (142). *E*, radioactivity release on Edman degradation of different segments of DAF-labeled DT in membranes (1–378).

served as seen in the B-chain helices, suggesting that primarily lipids surround this region (Fig. 3*D*). Therefore, this evidence strongly supports the hypothesis that the A-chain, extended outward with this region, provides the membrane-spanning region.

Endoproteinase Glu-C Digestion of Membrane-bound DT Labeled by DAF and Identification of Membrane-bound Fragments—In order to get information on sites labeled in the middle of the T domain (where there are no Met residues), the DAF-labeled DT vesicles were subjected to fragmentation by Endo-Glu-C. This permitted isolation of a vesicle-bound 14-kDa fragment by SDS-PAGE and electroblotting, and this fragment could be identified by peptide sequencing (LKLTVTG . . .) as the fragment resulting from cleavage at Glu^{262}. This peptide could be sequenced for 26 cycles allowing us to cover the TH5 helix, which has been suggested to be membrane-associated. The only discernible residue that was labeled in this region was Trp^{281}, and this residue was significantly labeled (Fig. 3*E*).

o-Iodosobenzoic Acid Fragmentation of Membrane-bound DT Labeled by DAF—The A-chain of DT has 2 tryptophan residues at positions 50 and 153. *o*-Iodosobenzoic acid is known to cleave proteins at Trp residues (49) and can thus provide fragments not accessible by CNBr cleavage. The A-chain was isolated from DAF-labeled membrane-bound DT by preparative electrophoresis followed by elution of the band corresponding to the A-chain using a extraction procedure involving sonication (44). The isolated labeled A-chain was then cleaved with *o*-iodosobenzoic acid. Analysis by SDS-PAGE found five bands corresponding to molecular masses of 15, 11, 7, and 4.5 kDa and part of an uncleaved A-chain at 23 kDa. After electroblotting, the 11- and 4.5-kDa bands were subjected to Edman degradation and could be identified as fragments corresponding to cleavage at Trp-50 (KGFYFSTDN . . ., 51–153) and Trp-153 (EQAKALSV . . . , 154–190). The 4.5-kDa fragment beginning with Glu^{154} indicated practically no labeling by counting the slice corresponding to this band on SDS-PAGE. This fragment could also be sequenced for 16 cycles, and a very low level of

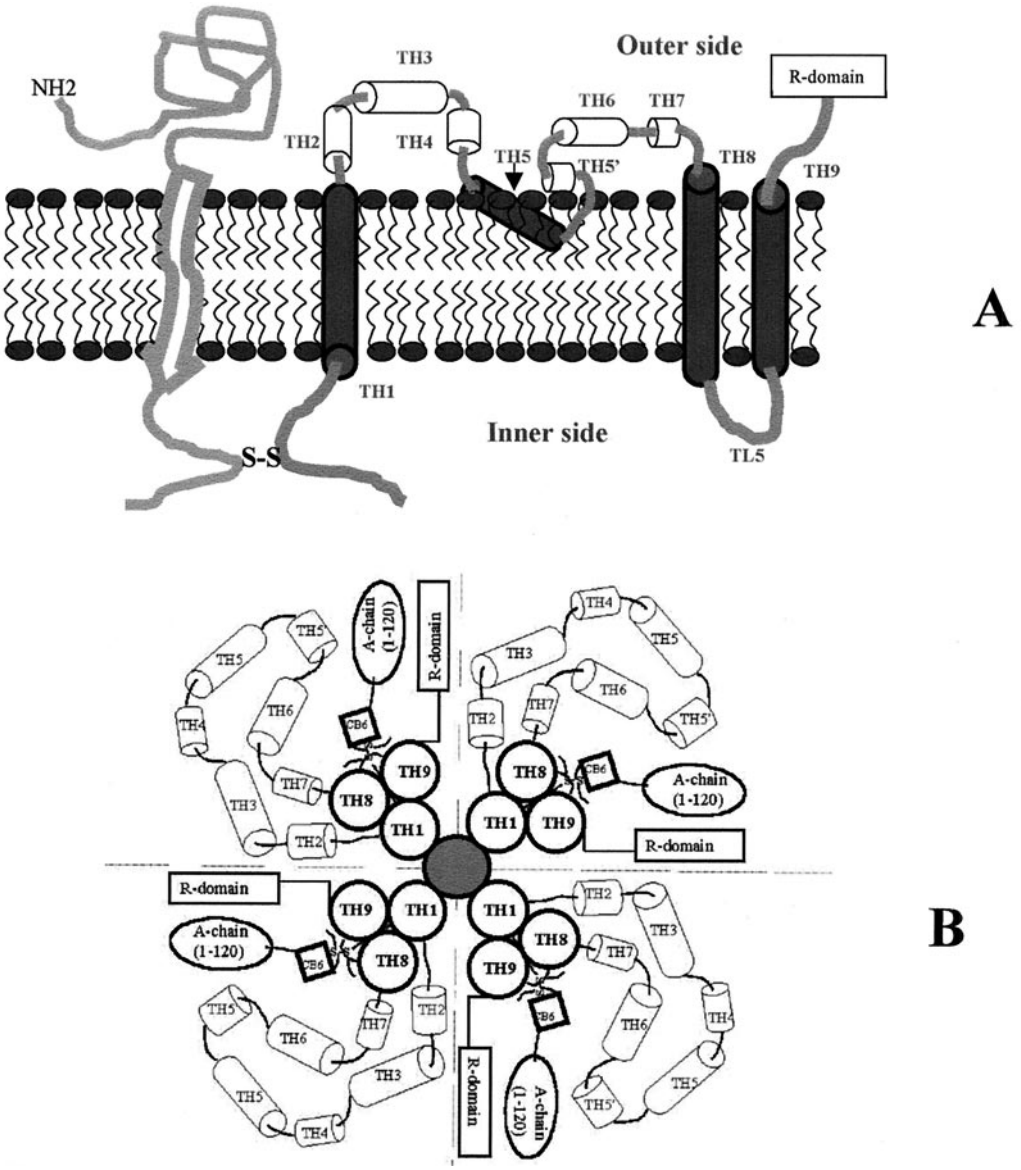

FIG. 4. *A*, topological model for DT insertion in model membranes. The α-helices TH1 to TH9 from the T domain and the β-sheet CB6 from the C domain refer to the structural motifs in the crystal structure of DT (5). The helices TH1, TH8, and TH9 and the β-strand CB6 are shown in transmembrane orientation. *B*, oligomeric state of DT in model membranes. The schematic top view shows the tetrameric model of the pore formed by DT in membranes. The *larger thick-walled central circle* represents the transmembrane toxin pore formed by TH1, TH8, and TH9 of the T domain. The *square* indicates the transmembrane β-strand (CB6) with disulfide facing toward the *trans* side.

radioactivity was found associated with the sequencing cycles (Fig. 3*E*). The second fragment (11 kDa) beginning with Lys^{51}, which encompasses the strongly labeled CB6 region (130–142), was found to be heavily labeled by SDS-PAGE. The sequencing of this fragment could be carried out for 26 cycles. However, a very low level of radioactivity was found associated with the sequencing cycles (Fig. 3*E*), indicating that this region of the DT is not labeled by DAF.

DISCUSSION

We have earlier reported that DAF can be used to map hydrophobic surfaces in proteins (37, 50, 51). Folding intermediates like the molten globule state, which involves a disrupted tertiary structure but a stable secondary structure leading to hydrophobic exposure, can be characterized by hydrophobic photolabeling with DAF. DAF binds to hydrophobic sites exposed by bovine α-lactalbumin in the molten globule state and labels it during photolysis (50). Similarly, DT, which is known to expose hydrophobic sites on lowering of pH is extensively photolabeled by DAF at pH 5.2 but not at pH 7.4. Analysis of DT labeled with DAF indicated that, although both A- and B-chains are labeled, it is only the B-chain that shows an increase in labeling when pH is lowered. More specifically, it was observed that the proposed membrane-penetrating hydrophobic helices TH8 and TH9 are extensively labeled (37).

In the present work we have shown that, if DAF is partitioned into a membrane, it labels the protein that inserts into the membrane and not the unbound soluble protein. In view of the fact that DAF is reported to label membrane-spanning regions of transmembrane protein (34, 35), an analysis of DAF-labeled sites permitted identification of membrane-spanning domains in membrane-bound DT. Both chemical and enzymatic fragmentation followed by separation and sequencing thus permitted identification of segments like TH8 and TH9, which have been suggested earlier as well as putative membrane-penetrating helices. Fig. 4*A* provides a likely model for membrane-inserted DT based on these results. In addition to the TH8-TH9 region, which is extensively labeled, it is interesting to note that the connecting TL5 loop is not labeled and is

thus suggested to be on the *trans* side. Sequencing of the 14-kDa fragment cleaved with Endo-Glu-C beginning with Leu^{263} for 26 cycles indicated major labeling only of Trp^{281} in this region, suggesting that the bulk of this part of DT lies on the outer side. The presence of a disulfide link on the *trans* side and no labeling in residues 142–173 and 194–206 suggest that this part of the molecule is on the *trans* side. Furthermore, the absence of any significant labeling in regions 15–76 and 116–133 suggests that the bulk of the A-chain lies on the outside (Fig. 4*A*). However, keeping in view the amphiphilic nature of the TH1 helix and labeling primarily of the hydrophobic surface (Fig. 4*A*), it is likely that the inserted toxin exists as an oligomer in the membrane (Fig. 4*B*) so that the TH8, TH9, and TH1 helices form a channel with the hydrophilic end of TH1 in the oligomer that constitutes the lumen of the channel. After the disulfide reduction, the A-chain could laterally move so that it can wriggle through the pore.

We conclude that both A- and B-chains of DT insert into membranes as the pH is lowered to the range found in endosomes (pH 5.2–5.8). Furthermore, some of the secondary structural elements of the solution structure are retained in the membrane-inserted state with protein-folding changes occurring primarily in the loop regions. Thus TH1, TH8, and TH9 observed in the T domain of the solution structure, not only insert into the membrane but also maintain their helical nature. It is very likely that DT exists as an oligomer in membranes (52) so that these helices can participate in forming a channel, which permits the partly embedded catalytic domain to transport through this channel after it is released by reduction of the disulfide group holding the two chains together. Similar transport phenomena of phage proteins have been described recently (53). The structural similarity between TH8 and TH9 helices and proteins (Bcl-x_L) involved in regulation of apoptosis (54) suggests that a similar translocation mechanism may be involved in other systems. Finally, the retention of secondary structural elements in the membrane-inserted state point toward the involvement of a molten globule state in DT. This state has been observed in many proteins as a folding intermediate, which has a disrupted tertiary structure but a stable secondary structure and increased hydrophobic exposure (55). It is important to note that increased hydrophobic exposure and formation of a molten globule-like intermediate at a pH value (5.2) close to that observed in endosomes have been detected in the case of DT and that their possible involvement in insertion into membranes has been found previously (37). A recent report points to the ability of proteins that can form a stable molten globule-like intermediate, to promote the translocation of DT (56). It is thus exciting to see the early hypothesis on involvement of the molten globule state of soluble proteins in providing a conformational state conducive to membrane entry begin to come to fruition (57). Finally, the methodology used here should make the study of insertion of other soluble proteins in membranes possible.

Acknowledgment—The mutated DT toxin strain was a generous gift from Dr. R. J. Collier, Harvard Medical School, Boston, MA.

REFERENCES

1. Pappenheimer, A. M., Jr. (1977) *Annu. Rev. Biochem.* **46,** 64–94
2. Collier, R. J. (1975) *Bacteriol. Rev.* **39,** 54–85
3. Lacy, D. B., and Stevens, R. C. (1998) *Curr. Opin. Struct. Biol.* **8,** 778–784
4. Choe, S., Bennett, M. J., Fujii, G., Curmi, P. M. G., Kantardjieff, K. A., Collier, R. J., and Eisenberg, D. (1992) *Nature* **357,** 216–222
5. Bennett, M. J., and Eisenberg, D. (1994) *Protein Sci.* **3,** 1464–1475
6. Sandvig, K., and Olsnes, S. (1980) *J. Cell Biol.* **87,** 828–832
7. Moskaug, J. O., Stenmark, H., and Olsnes, S. (1991) *J. Biol. Chem.* **266,** 2652–2659
8. Naglich, J. G., Metherall, J. E., Russell, D. W., and Eidels, L. (1992) *Cell* **69,** 1051–1061
9. Madshus, I. H., Wiedlocha, A., and Sandvig, K. (1994) *J. Biol. Chem.* **269,** 4648–4652
10. O'Keefe, D. O., Cabiaux, V., Choe, S., Eisenberg, D., and Collier, R. J. (1992) *Proc. Natl. Acad. Sci. U. S. A.* **89,** 6202–6206
11. Honjo, T., Nishizuka, Y., and Hayaishi, O. (1968) *J. Biol. Chem.* **243,** 3553–3555
12. Hu, V. W., and Holmes, R. K. (1984) *J. Biol. Chem.* **259,** 12226–12233
13. Silverman, J. A., Mindell, J. A., Finkelstein, A., Shen, W. H., and Collier, R. J. (1994) *J. Biol. Chem.* **269,** 22524–22532
14. Zhan, H., Choe, S., Huynh, P. D., Finkelstein, A., Eisenberg, D., and Collier, R. J. (1994) *Biochemistry* **33,** 11254–11263
15. Tortorella, D., Sesardic, D., Dawes, C. S., and London, E. (1995) *J. Biol. Chem.* **270,** 27439–27445
16. Tortorella, D., Sesardic, D., Dawes, C. S., and London, E. (1995) *J. Biol. Chem.* **270,** 27446–27452
17. Papini, E., Schiavo, G., Tomasi, M., Colombatti, M., Rappuoli, R., and Montecucco, C. (1987) *Eur. J. Biochem.* **169,** 637–644
18. Gonzales, J. E., and Weisnieski, B. J. (1988) *J. Biol. Chem.* **263,** 15257–15259
19. Umata, T., and Mekada, E. (1998) *J. Biol. Chem.* **273,** 8351–8359
20. Zhao, J. M., and London, E. (1988) *J. Biol. Chem.* **263,** 15369–15377
21. Quertenmont, P., Wolff, C., Wattiez, R., Vander Borght, P., Falmagne, P., Ruysschaert, J. M., and Cabiaux, V. (1999) *Biochemistry* **38,** 660–666
22. Asuncion Punzalan, E., Kachel, K., and London, E. (1998) *Biochemistry* **37,** 4603–4611
23. Kachel, K., Ren, J., Collier, R. J., and London, E. (1998) *J. Biol. Chem.* **273,** 22950–22956
24. Malenbaum, S. E., Collier, R. J., and London, E. (1998) *Biochemistry* **37,** 17915–17922
25. Oh, K. J., Zhan, H., Cui, C., Hideg, K., Collier, R. J., and Hubbell, W. L. (1996) *Science* **273,** 810–812
26. Oh, K. J., Zhan, H., Cui, C., Altenbach, C., Hubbell, W. L., and Collier, R. J. (1999) *Biochemistry* **38,** 10336–10343
27. Mindell, J. A., Silverman, J. A., Collier, R. J., and Finkelstein, A. (1994) *J. Membr. Biol.* **137,** 45–57
28. Mindell, J. A., Silverman, J. A., Collier, R. J., and Finkelstein, A. (1994) *J. Membr. Biol.* **137,** 29–44
29. Ren, J., Sharpe, J. C., Collier, R. J., and London, E. (1999) *Biochemistry* **38,** 976–984
30. Mindell, J. A., Zhan, H., Huynh, P. D., Collier, R. J., and Finkelstein, A. (1994) *Proc. Natl. Acad. Sci. U. S. A.* **91,** 5272–5276
31. Kaul, P., Silverman, J., Shen, W. H., Blanke, S. R., Huynh, P. D., Finkelstein, A., and Collier, R. J. (1996) *Protein Sci.* **5,** 687–692
32. Huynh, P. D., Cui, C., Zhan, H. J., Oh, K. J., Collier, R. J., and Finkelstein, A. (1997) *J. Gen. Physiol.* **110,** 229–242
33. Lala, A. K., Batliwala, H. F., and Bhat, S. (1990) *Pure Appl. Chem.* **62,** 1453–1456
34. Lala, A. K., and Bhat, S. (1990) *Biotechnol. Appl. Biochem.* **12,** 586–594
35. Pradhan, D., and Lala, A. K. (1987) *J. Biol. Chem.* **262,** 8242–8251
36. Lala, A. K., and Raja, S. M. (1995) *J. Biol. Chem.* **270,** 11348–11357
37. D'Silva, P. R., and Lala, A. K. (1998) *J. Biol. Chem.* **273,** 16216–16222
38. Lowry, O. H., Rosebrough, N. J., Farr, A. L., and Randall, R. J. (1951) *J. Biol. Chem.* **193,** 265–275
39. Eibl, H., McIntyre, J. O., Fleer, E. A. M., and Fleischer, S. (1983) *Methods Enzymol.* **98,** 623–632
40. Kallury, R. K., Krull, U. J., and Thompson, M. (1987) *J. Org. Chem.* **52,** 5478–5480
41. Ames, B. N., and Dubin, D. T. (1960) *J. Biol. Chem.* **235,** 769–775
42. Schagger, H., and Von Jagow, G. (1987) *Anal. Biochem.* **166,** 368–379
43. Mozdzanowski, J., and Speicher, D. W. (1992) *Anal. Biochem.* **207,** 11–18
44. Quertenmont, P., Wattiez, R., Falmagne, P., Ruysschaert, J. M., and Cabiaux, V. (1996) *Mol. Microbiol.* **21,** 1283–1296
45. Retamal, C. A., Thiebaut, P., and Alves, E. W. (1999) *Anal. Biochem.* **268,** 15–20
46. Papini, E., Colonna, R., Cusinato, F., Montecucco, C., Tomasi, M., and Rappuoli, R. (1987) *Eur. J. Biochem.* **169,** 629–635
47. Senzel, L., Huynh, P. D., Jakes, K. S., Collier, R. J., and Finkelstein, A. (1998) *J. Gen. Physiol.* **112,** 317–324
48. Oh, K. J., Senzel, L., Collier, R. J., and Finkelstein, A (1999) *Proc. Natl. Acad. Sci. U. S. A.* **96,** 8467–8470
49. Mahoney, W. C., and Hermodson, M. A. (1979) *Biochemistry* **18,** 3810–3814
50. D'Silva, P. R., and Lala, A. K. (1999) *Protein Sci.* **8,** 1099–1103
51. Lala, A. K., and Kaul, P. (1992) *J. Biol. Chem.* **267,** 19914–19918
52. Sharpe, J. C., and London, E. (1999) *J. Membr. Biol.* **171,** 209–221
53. Marciano, D. K., Russell, M., and Simon, S. M. (1999) *Science* **284,** 1516–1519
54. Muchmore, S. W., Sattler, M., Liang, H., Meadows, R. P., Harlan, J. E., Yoon, H. S., Nettesheim, D., Chang, B. S., Thompson, C. B., Wong, S. L., Ng, S. L., and Fesik, S. W. (1996) *Nature* **381,** 335–341
55. Ptitsyn, O. B. (1995) *Curr. Opin. Struct. Biol.* **5,** 74–78
56. Ren, J., Kachel, K., Kim, H., Malenbaum, S. E., Collier, R. J., and London, E. (1999) *Science* **284,** 955–957
57. Bychkova, V. E., Pain, R. H., and Ptitsyn, O. B. (1988) *FEBS Lett.* **238,** 231–234
58. Laemmli, U. K. (1970) *Nature* **227,** 680–685

THE JOURNAL OF BIOLOGICAL CHEMISTRY
Vol. 275, No. 35, Issue of September 1, p. 27500, 2000

Printed in U.S.A.

Additions and Corrections

Vol. 275 (2000) 11771–11777

Organization of diphtheria toxin in membranes: a hydrophobic photolabeling study.

Patrick R. D'Silva and Anil K. Lala

Page 11775: The abscissa in Fig. 3*E* should read 16, 66, 116, 166, 216, 266, 316, 366, instead of 1, 51, 101, 151, 201, 251, 301, 351

Vol. 275 (2000) 18919–18925

Cloning and characterization of the gene for phosphatidylcholine synthase.

Christian Sohlenkamp, Karel E. E. de Rudder, Viola Röhrs, Isabel M. López-Lara, and Otto Geiger

This article should be listed in category 2, "Genes: Structure and Regulation," rather than category 13, "Molecular Basis of Cell and Developmental Biology."

We suggest that subscribers photocopy these corrections and insert the photocopies at the appropriate places where the article to be corrected originally appeared. Authors are urged to introduce these corrections into any reprints they distribute. Secondary (abstract) services are urged to carry notice of these corrections as prominently as they carried the original abstracts.